High-Resolution Photocurrent Mapping of Carbon Nanostructures

Marko Burghard[†] and Alf Mews[‡,*]

[†]Max Planck Institute for Solid State Research, Heisenbergstrasse 1, D-70569 Stuttgart, Germany and [‡]Institute of Physical Chemistry, University of Hamburg, Grindelallee 117, D-20146 Hamburg, Germany

ABSTRACT

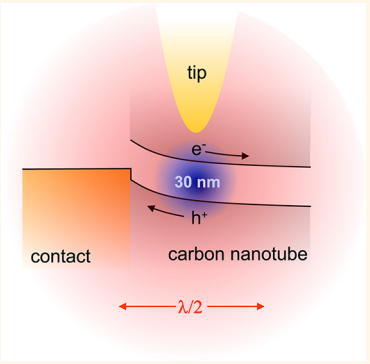

The spatial resolution of photocurrent measurements on carbon nanostructures has reached 20 nm, as demonstrated by Hartschuh and co-workers for individual carbon nanotubes in this issue of *ACS Nano*. In this Perspective, we provide a brief overview of the applications of scanning photocurrent microscopy to various one- and two-dimensional nanostructures and highlight the importance of the optical antenna concept for future studies of the optoelectronic properties of hybrid nanostructures.

Photocurrent generation is a key process in a range of technologically relevant devices, in particular, solar cells and photodetectors. One method used to investigate the solar cells' spatial uniformity in terms of electrical performance is a technique called laser-beam-induced current (LBIC), which was developed in the early 1980s.[1] In this technique, a focused laser beam performs a two-dimensional scan of the photoactive surface of the device, while measuring the generated short circuit photocurrent. Thus, images of the photoconversion efficiency of the scanned surface are obtained, with spatial resolution governed by the size of the laser spot. These images can be directly correlated with structural information provided by other image-capturing techniques such as optical or electronic microscopy.[2]

With the advent of efficient chemical synthesis methods for carbon or inorganic semiconductor-based nanostructures, a slight variation of the LBIC technique, scanning photocurrent microscopy (SPCM), emerged as a versatile diagnostic tool to explore the electronic properties of individual nanotubes or nanowires. The pioneering experiments revealed the presence of photocurrent signals at the metal contacts to individual semiconducting single-wall carbon nanotubes (SWCNTs),[3] whose magnitude is controllable by the application of a back gate voltage,[4−6] which is known to modulate the height of the Schottky barriers at these locations. Further SPCM studies focused on determining built-in electric fields at the metal contacts to metallic SWCNTs[7] or SWCNT interconnections.[8] In parallel, the application of SPCM was expanded to inorganic semiconductor nanowires,[9] providing useful information such as the electric field dependence of the photocurrent decay length.[10] Besides the one-dimensional carbon nanotubes, SPCM was then also applied to their two-dimensional counterpart, graphene. The first experiments along this line examined the potential steps formed at the metal contacts.[11] However, the spatial resolution in the above-described SPCM experiments was always restricted to the diffraction-limited spot size of the laser ($\geq\lambda/2$), which prevented the evaluation of the electric potential variations on the nanoscale. As a first step toward increased spatial resolution, Avouris and co-workers reported in 2009 scanning near-field optical microscope (SNOM)-based SPCM measurements on graphene.[12] In this manner, spatial resolution of ~50 nm could be reached, which opened the possibility to probe the interfaces between single-layer and multilayered graphene regions.

A further leap in terms of spatial resolution of SPCM has now been attained by Rauhut *et al.* for individual carbon nanotubes, as described in this issue of *ACS Nano*.[13]

* Address correspondence to mews@chemie.uni-hamburg.de.

Published online July 10, 2012
10.1021/nn3029088

A further leap in terms of spatial resolution of scanning photocurrent microscopy has now been attained by Rauhut *et al.* for individual carbon nanotubes, as described in this issue of *ACS Nano*.

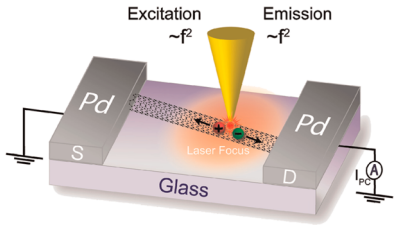

Figure 1. Scheme of the tip-enhanced photocurrent microscopy setup as used by Rauhut *et al*. Reprinted from ref 13. Copyright 2012 American Chemical Society. The photocurrent through contacted carbon nanotubes is monitored as a function of the illumination position. By using a sharp metallic tip as an antenna to enhance the light field in a small volume, changes in the electric field along the tube with extensions of just a few tens of nanometers can be resolved.

They utilize the so-called apertureless near-field technique, where a sharp metal tip acting as a nanoscopic antenna is brought into close proximity to the sample. The antenna effect is based on the collective motion of the free electrons within the metallic tip, which are resonantly excited by laser irradiation. These plasmonic oscillations strongly increase the electromagnetic field strength up to a few nanometers away from the tip surface. Accordingly, strong light interaction is limited to the proximity of the tip, enabling spatial resolution for optical excitation that is governed mainly by the size of the tip. This is superior by approximately 1 order of magnitude in comparison to confocal microscopy methods such as scanning confocal Raman microscopy[14] or fluorescence microscopy and spectroscopy,[15] which have been successfully employed to distinguish between metallic and semiconducting nanotubes and even to determine the helical index of individual carbon nanotubes.[16] As early as 2003, Hartschuh *et al.* used tip-enhanced near-field optical microscopy (TENOM) to increase the spatial resolution of fluorescence and Raman microscopies. In these experiments, they could observe fluorescing segments of nanotubes, which were only a few tens of nanometers in length and were attributed to chirality changes along the tube axis.[15] Now, they have combined tip-enhanced Raman and photocurrent microscopy, which can even be measured simultaneously (Figure 1).[13] This enables direct comparisons between the signal intensity and spatial resolution in the Raman and SPCM measurements, which provides useful information about the underlying physical enhancement mechanisms. Interestingly, they observed the spatial width of the Raman signals (~20 nm) to be narrower than the width of the respective SPCM signals (~30 nm). To explain this difference, Rauhut *et al.* suggest that, in Raman scattering, the antenna effect enhances both the excitation and also the emission rate, whereas in SPCM, only the excitation rate is enhanced. Accordingly, the width of the Gaussian excitation cross section should theoretically be smaller by a factor of $\sqrt{2}$ for the Raman signal, which is in perfect agreement with the experimental observations.

The tip-enhanced SPCM enabled Rauhut *et al.* to gain deeper insight into the photocurrent generation mechanism in carbon nanostructures. Recently, it has been discussed that, besides the built-in electric field, the thermoelectric effect represents another mechanism of photocurrent generation, based on SPCM studies on graphene.[17] The latter involves the formation of a temperature gradient ΔT due to local heating by the laser, which produces a thermoelectric voltage given by $V = S \times \Delta T$ (where S is the Seebeck coefficient). While thus far, no general consensus has been attained as to which of the two mechanisms dominates, the data obtained by Rauhut *et al.* support the built-in field mechanism for two reasons. First, with increased optical resolution, they were able to show that the energy band profile obtained by integrating the photocurrent signal along the nanotube decays exponentially along the length of the nanotube, in close agreement with theoretical predictions. Second, they observed a sign change in the signal far away from the metal contacts that could not be explained by local laser heating of the nanotube nor by (indirect) heating of the electrodes. However, it should be noted that the situation may well be different for the photoresponse close to the metal contacts. Indeed, according to a recent confocal-microscopy-based study on networks of SWCNTs, the contact-related photoresponse mainly arises from temperature variations at the metal–nanotube interface.[18] In addition, the photoresponse has been found to be influenced by the device operation regime, the type of substrate, as well as postgrowth treatment of the nanotubes.

Another interesting aspect of tip-enhanced SPCM is the ability to explore the effects of local perturbations along the nanotube axis. For example Rauhut *et al.* observed for some samples that the sign of the SPCM signal changed on length scales of only a few tens of nanometers. Possible origins for this behavior involve local structural

defects of the CNTs or electrostatic perturbations from the environment of the nanotubes. By taking advantage of the combined microscopic information, they could identify charged particles in close proximity to the nanotube as the most likely cause of the photocurrent features. This conclusion is based on the finding that the photocurrent signatures always coincide with the presence of a small particle at the same position in the acquired topography image. Further support could be gained from the simultaneously recorded intensity of the so-called defect Raman mode (D-band), which is a measure of the local structural defect density. In particular, the absence of correlations between the local defect density and the spatial photocurrent modulation suggests that the latter is due to band bending resulting from electrostatic interactions with the attached particles.

Another interesting aspect of tip-enhanced scanning photocurrent microscopy is the ability to explore the effects of local perturbations along the nanotube axis.

OUTLOOK AND FUTURE CHALLENGES

The use of antenna effects represents a highly attractive approach that is applicable more broadly to other nanostructures. Along these lines, it has been demonstrated that, by attaching plasmonic nanostructures (*e.g.*, lithographically defined gold dot patterns) to graphene, the efficiency of graphene p–n junction photodetectors can be increased up to 20-fold.[19] Furthermore, with the aid of nanostructures of different geometries, it has been possible to impart wavelength and polarization selectivity to such devices. On a similar basis, photocurrent enhancement has recently been achieved for inorganic nanowires. Here, the polarization sensitivity and charge carrier generation in a 50 nm Si nanowire could be tailored by decorating its surface with plasmonic Au nanoparticles.[20] The local photocurrent enhancement observed in such samples has been assigned to the plasmonic near-field response of the individual nanoparticles, complemented by broad-band enhancement due to surface-enhanced optical absorption.

As an extension of separated metal dots or particles, so-called plasmonic clusters[21] emerge as ideal candidate structures for amplifying the optical response of graphene. Such clusters exhibit a transparency window where scattering is suppressed and hot electron–hole pair generation is the dominant light absorption mechanism. The associated strong enhancement of the near-field[22] has recently been exploited for the direct excitation of electron–hole pairs in a graphene monolayer in direct proximity to the plasmonic clusters.[23] By collecting the light-induced conduction electrons in graphene, efficient photodetectors can be obtained. The reported photodetector devices, consisting of an array of gold nanoparticle heptamers sandwiched between two graphene layers, have enabled the conversion of visible and near-infrared photons into electrons with an 8-fold enhancement of the photocurrent, as compared to graphene devices without antennas. Moreover, the spectral sensitivity of the devices could be tuned by the geometry of the plasmonic antenna as well as the application of a gate bias. A similar strategy to control the

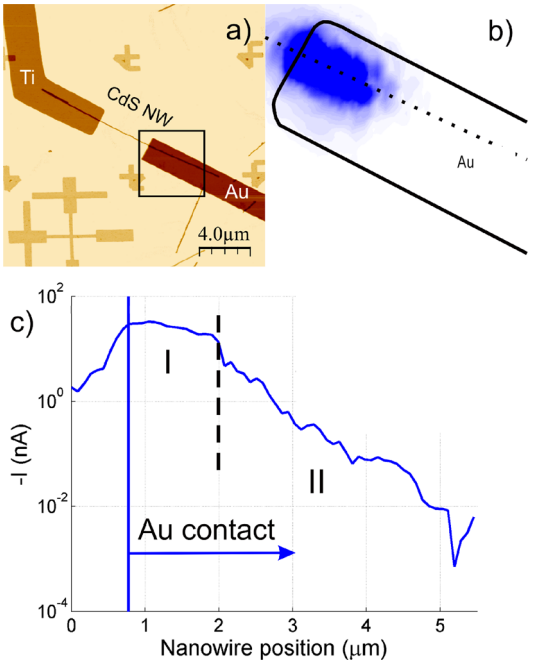

Figure 2. Spatially resolved photocurrent response of a gold-coated CdS nanowire segment. Reprinted from ref 25. Copyright 2012 American Chemical Society. (a) Atomic force microscopy image of the nanowire (diameter of ~50 nm) contacted by one gold and one titanium electrode, separated by a few nanometers. The black frame marks the area where the photocurrent map in panel (b) was recorded (λ_{laser} = 488 nm). The electrode edges are highlighted by a black solid line. (c) Photocurrent profile along the dotted line in panel (b). In the first regime (I), the photocurrent is almost constant, whereas in the second regime (II), an approximately linear decrease in photocurrent with increasing distance from the electrode edge is observed. Regimes I and II are attributable to drift and diffusion currents, respectively.

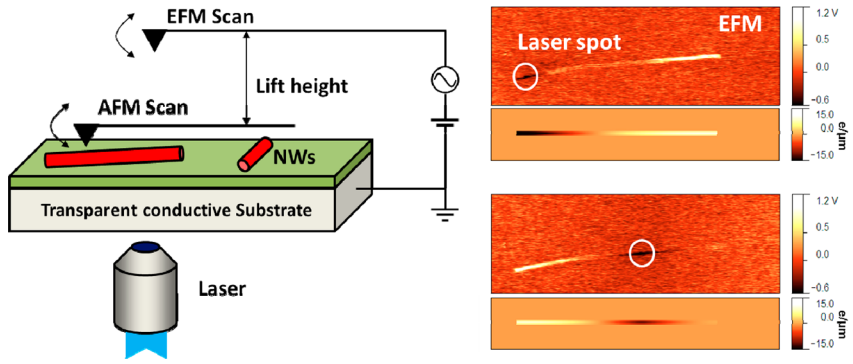

Figure 3. Measurement of the charge distribution in CdSe semiconductor nanowires upon local laser illumination. Reprinted from ref 27. Copyright 2011 American Chemical Society. The nanowires are excited with a focused laser spot (λ_{laser} = 488 nm) in a confocal microscope, and the resulting charge imbalance is imaged by electrostatic force microscopy (EFM) at the same time. In the respective EFM images (upper graphs) and EFM simulations (lower graphs), a bright color corresponds to positive charging while a dark color corresponds to negative charging. Because photogenerated electrons and holes have different mobilities within the one-dimensional nanowire, the electrons spread almost uniformly along the wire, whereas the holes are more localized at the excitation spot. This leads to positive excess charges at the excitation spot.

light–matter interactions in graphene involves its implementation into an optical microcavity.[24] The microcavity-induced optical confinement yields a 20-fold enhancement of photocurrent, combined with the capability to control both the thermal light emission from graphene and the electrical transport characteristics of an integrated graphene transistor.

In addition to antenna-based devices, the scanning photocurrent microscopy response of inorganic nanowires or carbon nanostructures below the metal contacts deserves further attention.

In addition to antenna-based devices, the SPCM response of inorganic nanowires or carbon nanostructures below the metal contacts deserves further attention. For instance, it has recently been found that the photoresponse of the Schottky-type contact between gold and a CdS nanowire contains spatially separate contributions of diffusion and drift currents (Figure 2).[25] This has enabled the determination of the electron diffusion length and recombination rate in the metal-coated nanowire section. Moreover, evidence has been gained that the charge carriers can be efficiently extracted out of the contacts, which has implications for the further development of nanowire-based solar cells or photodetectors. In the case of gold-coated graphene, the photoresponse has provided evidence that the electronic structure, the electron–phonon coupling, and the doping level are largely preserved.[26] Further, the transfer lengths for electrons and holes at the graphene–gold contact could be determined to be as high as 1.6 μm, which poses limitations on the scaling of gold contacts within graphene devices.

The aforementioned examples highlight a wide variety of physical effects that are observable in hybrid nanostructures. These effects can lead to a wide range of new materials properties, opening numerous possible applications. In this respect, the work of Rauhut *et al.* underscores that detailed knowledge of the physical effects is required to develop new analytical tools for the nanoscale. At the same time, it becomes apparent that only combinations of several different techniques such as confocal optical microscopy and spectroscopy enhanced by nanoscopic antennas, as well as topography measurements and electronic transport experiments, are adequate to explore the details of complex nanoscopic devices. An additional direction is to use the tip as a tool to measure the local electronic properties. To mention just two examples, electrostatic force microscopy (EFM) is well-suited to probe the charge distribution along semiconductor nanowires (Figure 3),[27] and Kelvin probe force microscopy (KPFM) enables direct monitoring of the potential profile along nanostructures.[28] Additionally, the local probes could be used to manipulate the electronic properties of individual nanostructure, either by local injection of charges or by applying local electrostatic field.

Conflict of Interest: The authors declare no competing financial interest.

REFERENCES AND NOTES

1. Marek, J. Light-Beam Induced Current Characterization of Grain Boundaries. *J. Appl. Phys.* **1984**, *55*, 318–326.
2. Vorster, F. J.; van Dyk, E. E. Bias-Dependent High Saturation Solar LBIC Scanning of Solar Cells. *Sol. Energy Mater. Sol. Cells* **2007**, *91*, 871–876.
3. Balasubramanian, K.; Fan, Y. W.; Burghard, M.; Kern, K.; Friedrich, M.; Wannek, U.; Mews, A. Photoelectronic Transport Imaging of Individual Semiconducting Carbon Nanotubes. *Appl. Phys. Lett.* **2004**, *84*, 2400–2402.
4. Balasubramanian, K.; Burghard, M. Charge Transport through Carbon Nanotubes Interacting with Light. *Semicond. Sci. Technol.* **2006**, *21*, S22–S32.

5. Freitag, M.; Tsang, J. C.; Bol, A.; Yuan, D. N.; Liu, J.; Avouris, P. Imaging of Schottky Barriers and Charge Depletion in Carbon Nanotube Transistors. *Nano Lett.* **2007**, *7*, 2037–2042.
6. Lee, E. J. H.; Balasubramanian, K.; Dorfmüller, J.; Vogelgesang, R.; Fu, N.; Mews, A.; Burghard, M.; Kern, K. Electronic-Band-Structure Mapping of Nanotube Transistors by Scanning Photocurrent Microscopy. *Small* **2007**, *3*, 2038–2042.
7. Balasubramanian, K.; Burghard, M.; Kern, K.; Scolari, M.; Mews, A. Photocurrent Imaging of Charge Transport Barriers in Carbon Nanotube Devices. *Nano Lett.* **2005**, *5*, 507–510.
8. Lee, E. J. H.; Balasubramanian, K.; Burghard, M.; Kern, K. Spatially Resolved Potential Distribution in Carbon Nanotube Cross-Junction Devices. *Adv. Mater.* **2009**, *21*, 2720–2724.
9. Ahn, Y.; Dunning, J.; Park, J. Scanning Photocurrent Imaging and Electronic Band Studies in Silicon Nanowire Field Effect Transistors. *Nano Lett.* **2005**, *5*, 1367–1370.
10. Graham, R.; Miller, C.; Oh, E.; Yu, D. Electric Field Dependent Photocurrent Decay Length in Single Lead Sulfide Nanowire Field Effect Transistors. *Nano Lett.* **2011**, *11*, 717–722.
11. Lee, E. J. H.; Balasubramanian, K.; Weitz, R. T.; Burghard, M.; Kern, K. Contact and Edge Effects in Graphene Devices. *Nat. Nanotechnol.* **2008**, *3*, 486–490.
12. Mueller, T.; Xia, F.; Freitag, M.; Tsang, J.; Avouris, P. Role of Contacts in Graphene Transistors: A Scanning Photocurrent Study. *Phys. Rev. B* **2009**, *79*, 245430.
13. Rauhut, N.; Engel, M.; Steiner, M.; Krupke, R.; Avouris, P.; Hartschuh, A. Antenna-Enhanced Photocurrent Microscopy on Single-Walled Carbon Nanotubes at 30 nm Resolution. *ACS Nano* **2012**, 10.1021/nn301979c.
14. Mews, A.; Koberling, F.; Basche, T.; Philipp, G.; Duesberg, G. S.; Roth, S.; Burghard, M. Raman Imaging of Single Carbon Nanotubes. *Adv. Mater.* **2000**, *12*, 1210–1214.
15. Hartschuh, A.; Pedrosa, H. N.; Novotny, L.; Krauss, T. D. Simultaneous Fluorescence and Raman Scattering from Single Carbon Nanotubes. *Science* **2003**, *301*, 1354–1356.
16. Hartschuh, A.; Qian, H.; Meixner, A. J; Anderson, N.; Novotny, L. Nanoscale Optical Imaging of Excitons in Single-Walled Carbon Nanotubes. *Nano Lett.* **2005**, *5*, 2310–2313.
17. Park, J.; Ahn, Y. H.; Ruiz-Vargas, C. Imaging of Photocurrent Generation and Collection in Single-Layer Graphene. *Nano Lett.* **2009**, *9*, 1742–1746.
18. St-Antoine, B. C.; Ménard, D.; Martel, R. Photothermoelectric Effects in Single-Walled Carbon Nanotube Films: Reinterpreting Scanning Photocurrent Experiments. *Nano Res.* **2012**, *5*, 73–81.
19. Echtermeyer, T. J.; Britnell, L.; Jasnos, P. K.; Lombardo, A.; Gorbachev, R .V.; Grigorenko, A. N.; Geim, A. K.; Ferrari, A. C.; Novoselov, K. S. Strong Plasmonic Enhancement of Photovoltage in Graphene. *Nat. Commun.* **2011**, *2*, 458.
20. Hyun, J. K.; Lauhon, L. J. Spatially Resolved Plasmonically Enhanced Photocurrent from Au Nanoparticles on a Si Nanowire. *Nano Lett.* **2011**, *11*, 2731–2734.
21. Lukyanchuk, B.; Zheludev, N. I.; Maier, S. A.; Halas, N. J.; Nordlander, P.; Giessen, H.; Chong, C. T. The Fano Resonance in Plasmonic Nanostructures and Metamaterials. *Nat. Mater.* **2010**, *9*, 707–715.
22. Stockman, M. I. Nanoscience: Dark-Hot Resonances. *Nature* **2010**, *467*, 541–542.
23. Fang, Z.; Liu, Z.; Wang, Y.; Ajayan, P. M.; Nordlander, P.; Halas, N. J. Graphene-Antenna Sandwich Photodetector. *Nano Lett.* **2012**, 10.1021.nl301774e.
24. Engel, M.; Steiner, M.; Lombardo, A.; Ferrari, A. C.; von Löhneysen, H.; Avouris, P.; Krupke, R. Light−Matter Interaction in a Microcavity-Controlled Graphene Transistor. *Nat. Commun.* **2012**, 10.1038/ncomms1911.
25. Dufaux, T.; Burghard, M.; Kern, K. Efficient Charge Extraction out of Nanoscale Schottky Contacts to CdS Nanowires. *Nano Lett.* **2012**, *12*, 2705–2709.
26. Sundaram, R. S.; Steiner, M.; Chiu, H.-Y.; Engel, M.; Bo, A. A.; Krupke, R.; Burghard, M.; Kern, K.; Avouris, P. The Graphene−Gold Interface and Its Implications for Nanoelectronics. *Nano Lett.* **2011**, *11*, 3833–3837.
27. Schäfer, S.; Wang, Z.; Zierold, R.; Kipp, T.; Mews, A. Laser-Induced Charge Separation in CdSe Nanowires. *Nano Lett.* **2011**, *11*, 2672–2677.
28. Koren, E.; Rosenwaks, Y.; Allen, J. E.; Hemesath, E. R.; Lauhon, L. J. Nonuniform Doping Distribution Along Silicon Nanowires Measured by Kelvin Probe Force Microscopy and Scanning Photocurrent Microscopy. *Appl. Phys. Lett.* **2009**, *95*, 092105.